J Therm Anal Calorim (2011) 105:61–71
DOI 10.1007/s10973-011-1546-1

Crystal structures and thermal properties of some rare earth alkoxides with tertiary alcohols

Possible precursors for atomic layer deposition of rare earth oxides

Timo Hatanpää · Kaupo Kukli · Mikko Ritala · Markku Leskelä

Niinistö"s Special Chapter

Abstract Rare earth (RE) alkoxides of Y, La, Pr, and Gd were synthesized using three tertiary alcohols namely 2,3-dimethyl-2-butanol, 2,2-dimethyl-3-ethyl-3-pentanol, and 3-isopropyl-2,4-dimethyl-pentan-3-ol. ^{1}H and ^{13}C NMR, elemental analysis (CHN) and MS were used to characterize the complexes. New crystal structures of dimeric $[Y(OCEt_2{}^tBu)_3]_2$, $[La(OCEt_2{}^tBu)_3]_2$, $[Gd(OC^iPr_3)_3]_2$, and $[La(OC^iPr_3)_3]_2$ were solved. Thermal properties of these compounds were studied with TG/SDTA and vacuum sublimation experiments. With all the cations Y, La, Pr, and Gd, the compounds with smallest ligand $^iPrMe_2CO^-$ seem to be the most volatile. The compounds with larger alkoxo ligands have lower volatility but their thermal stability is better. Atomic layer deposition experiments showed that RE oxide thin films could be grown from these alkoxides using water as the oxygen precursor.

Keywords Rare earth metals · Alkoxides · TG · ALD precursors

Introduction

Rare earth (RE) oxide thin films have received much attention because they are potential high-k oxides to replace SiO_2 in microelectronics [1, 2]. In such an application, the films have to be deposited conformally into complex structures and uniformly over large area substrates. These requirements make atomic layer deposition (ALD) an attractive method for high-k oxide deposition. ALD is a special CVD method in which the precursors are pulsed alternately one at the time onto the substrate and the growth proceeds via reactions between the adsorbed surface species and the incoming reactants [3]. The precursors have to meet three basic requirements: they must be volatile, they should not decompose when adsorbing on the surface and they should react aggressively with the other precursor needed to achieve the desired film composition. The last two requirements are often contradictory.

The most well-known precursor compounds for RE metals in CVD are β-diketonates. However, in the conventional ALD oxide processes with water as the other precursor, β-diketonates have often demonstrated too low reactivity against water [4, 5] which is most likely due to strong bonding (chelate effect) between the metal and the ligand, and also due to good sterical shielding of the ionic metal to oxygen bonds by the large β-diketonate ligands. Even if the films are deposited from β-diketonate with ozone as an oxygen precursor, the resulting films may contain considerable amounts of carbon, as shown in the case of Gd_2O_3 [6] and La_2O_3 [7]. The growth rates are also low. Recently, RE oxides have been deposited by ALD also using donor-functionalized alkoxides, amidinates, silylamides, and cyclopentadienyl compounds [4]. Donor-functionalized alkoxides introduced so far have been well volatile but have suffered from low thermal stability [8]. For amidinates details on the growth behavior, film composition and properties are still limited [9]. It has also been reported that water-based La_2O_3 processes lead to lanthanum hydroxide phases which continuously desorb water under deposition conditions to give a non-ALD growth pathway and poor film quality [10]. $Er(^tBuNCMeN^tBu)_3$

T. Hatanpää (✉) · K. Kukli · M. Ritala · M. Leskelä
Laboratory of Inorganic Chemistry, University of Helsinki, P. O. Box 55, 00014 Helsinki, Finland
e-mail: timo.hatanpaa@helsinki.fi

has been used with ozone to deposit Er_2O_3 but the film growth was not entirely self-limiting, as shown by a small increase in growth rate with increasing precursor dose [11]. Processes using silylamides and H_2O as oxygen precursor suffer from thermal decomposition of the silylamides and high amounts of silicon impurities in the films [4]. Several ALD processes using RE cyclopentadienyl compounds and water or ozone have been reported [4, 12]. With water RE oxide films can be grown with high growth rates at sufficiently low temperatures. In general also the film quality seems to be better as compared with the films prepared using RE β-diketonate/O_3 processes. Drawback of the unsubstituted cyclopentadienyl compounds is their generally lower thermal stability compared to, e.g., β-diketonates.

While new precursor classes have been introduced, some old possibilities like simple alkoxides with tertiary alkoxy ligands have gained no attention. They may have been ignored because in conventional CVD they have been found to be less suitable than for example β-diketonates or donor-functionalized alkoxides which, however, are far from optimal precursors for ALD [4]. Alkoxides of RE metals with small ligands like EtO^-, $^iPrO^-$, and $^tBuO^-$ are oligomeric compounds (pentameric–trimeric) with fairly low volatility and thermal stability [13–18]. Some alkoxides with tertiary alkoxo ligands larger than *t*-butoxo have been shown to be much more volatile and thermally stable [17, 18]. For example sublimation temperatures of 135–170 °C/10^{-3} torr reported for some Y and La alkoxides [17] suggest that vapor pressures sufficiently high for efficient film deposition can be achieved. Also because of the absence of chelate effect and less sterical shielding, higher reactivity with water vapor compared to β-diketonates and donor-functionalized alkoxides can be expected.

Some time ago we published a study on ALD of Gd_2O_3 using gadolinium alkoxide, $Gd(OCMe_2{}^iPr)_3$, and water as precursors [19]. It was found that Gd_2O_3 grew and started to crystallize at substrate temperatures as low as 250 °C. Films could be grown in a temperature range of 250–400 °C and more detailed study was performed at 400 °C. The growth rate varied between 0.34 and 0.49 Å per cycle against temperature. No systematic variations in the growth rate were observed when the Gd precursor pulse length was varied between 0.4 and 2 s, although pulses longer than 1 s caused significant scatter in the growth rate and refractive index [19]. The results suggested self-limiting growth at quite high temperatures, and considerable resistance of the precursor against thermal decomposition. The films were somewhat oxygen deficient and contained residual carbon and hydrogen, still crystallizing as cubic Gd_2O_3 in the as-deposited state at markedly low processing temperatures. In the films grown at 250 and 300 °C, some contribution from monoclinic Gd_2O_3 could also be detected. Films with thicknesses between 2.2 and 90 nm were grown. The permittivity of the thinnest films was 15.6 and that of thicker Gd_2O_3 films in the range of 17–19 [19].

In this work La, Pr, Gd, and Y alkoxides were synthesized using three tertiary alcohols namely 2,3-dimethyl-2-butanol ($HOCMe_2{}^iPr$), 2,2-dimethyl-3-ethyl-3-pentanol ($HOCEt_2{}^tBu$), and 3-isopropyl-2,4-dimethyl-pentan-3-ol (HOC^iPr_3). The compounds were characterized with NMR and MS. Thermal properties of the compounds were studied with TG/single differential thermal analysis (SDTA) measurements and vacuum sublimation experiments. Crystal structures of four new compounds, $[Y(OCEt_2{}^tBu)_3]_2$, $[La(OCEt_2{}^tBu)_3]_2$, $[Gd(OC^iPr_3)_3]_2$, and $[La(OC^iPr_3)_3]_2$ were solved. In addition, some ALD deposition studies with H_2O at the oxygen precursor were done.

Experimental

All manipulations were done under rigorous exclusion of air and moisture using standard Schlenk and glove box techniques. Anhydrous YCl_3 and $GdCl_3$ (99.99%) purchased from Aldrich and Strem were used as received. Anhydrous $LaCl_3$ (99.9%) purchased from Strem was converted to THF adduct before further usage by refluxing it in THF for 1 day. Hexamethyldisilazane (HMDS, $(Me_3Si)_2NH$) (≥98.0%) was received from Fluka and 2,3-dimethyl-2-butanol (99+%) from Aldrich. Alcohols 2,2-dimethyl-3-ethyl-3-pentanol and 3-isopropyl-2,4-dimethyl-pentan-3-ol were prepared using the methods described earlier [20, 21]. THF was freshly distilled over bentsophenone ketyl. Toluene was dried over 4 Å molecular sieves. Silylamides of Y, Gd, and La were prepared as described in the literature [22] by reacting the chlorides with potassium or lithium silylamide in THF. $Pr(N(SiMe_3)_2)_3$ was from Inorgtech.

CHN analyses were done in the Faculty of Pharmacy at University of Helsinki. ^1H and ^{13}C NMR spectra were recorded with a Varian Gemini 2000 instrument at ambient temperature. Chemical shifts were referenced to $SiMe_4$ and are given in ppm. Mass spectra were recorded with a JEOL JMS-SX102 operating in electron impact mode (70 eV) using a direct insertion probe and sublimation temperature range of 50–370 °C. A Mettler Star^e system equipped with a TGA 850 thermobalance was used for the thermal analyses of the samples. Flowing N_2 atmosphere was used. In dynamic experiments the heating rate was 10 °C/min and the samples investigated were between 9 and 12 mg. If observed, melting points were taken from the SDTA data measured by the thermobalance. A special heating program was used for isothermal mass change determination for $La(OCMe_2{}^iPr)_3$. The sample was heated to a desired temperature (230 °C) and then kept at this temperature for

15 min. Then the temperature was raised by 20 °C and the 15 min isothermal change was repeated. The highest temperature studied was 290 °C.

Preparation of $Y(OCMe_2{}^iPr)_3$ (**1**). 0.78 g of 2,3-dimethyl-2-butanol was added to 1.453 g (2.548 mmol) of $Y[N(SiMe_3)_2]_3$ dissolved in 50 mL of toluene. The solution was allowed to stir for 3 h after which the solution was evaporated to dryness and dried for 12 h under vacuum at 60 °C to remove all liberated HMDS. M.p. 164–171 °C. Yield was 90%. Anal. Calcd. for $Y_1O_3C_{18}H_{39}$ (392.406): C: 55.10; H: 10.02. Found: C: 53.61; H: 9.48. ^{1}H NMR (C_6D_6); 1.06 (d, 18H, CH_3), 1.32 (s, 18H, CH_3), 1.64 (sept., 3H, CH); $^{13}C\{^1H\}$ NMR (C_6D_6) 18.61 (CH_3), 29.38 (CH_3), 40.51 (CH), 75.76 (C). MS (EI, 70 eV) *m/z* 683 $[Y_2L_5]^+$.

All the other alkoxides were synthesized using a similar method to that used for $Y(OCMe_2{}^iPr)_3$. In the following only the analysis results are given for the other alkoxides.

$Gd(OCMe_2{}^iPr)_3$ (**2**). Yield: 87%. Anal. Calcd. for $Gd_1O_3C_{18}H_{39}$ (460.750): C: 46.83, H: 8.52. Found C: 46.68; H: 8.69. MS (EI, 70 eV) *m/z* 821 $[Gd_2L_5]^+$, 777 $[Gd_2L_4OCMeCH_2]^+$, 635 $[Gd_2L_3O]^+$.

$La(OCMe_2{}^iPr)_3$ (**3**). Yield: 96%. M.p. 116–126 °C. ^{1}H NMR (C_6D_6); 1.07 (d, 18H, CH_3), 1.41 and 1.44 (s, 18H, CH_3), 2.00 (sept., 3H, CH); $^{13}C\{^1H\}$ NMR (C_6D_6) 19.55 (CH_3), 28.82 (CH_3), 40.73 (CH), 77.22(C). MS (EI, 70 eV) *m/z* 783 $[La_2L_5]^+$.

$Pr(OCMe_2{}^iPr)_3$ (**4**).Yield: 95%. M.p. 83–93 °C. Anal. Calcd. for $Gd_1O_3C_{18}H_{39}$ (460.750): C: 48.65; H: 8.85. Found C: 47.17, H: 8.71. MS (EI, 70 eV) *m/z* 787 $[Pr_2L_5]^+$.

$Y(OCEt_2Bu^t)_3$ (**5**). Yield: 96%. M.p. 212–216 °C. Anal. Calcd. for $Y_1O_3C_{27}H_{57}$ (518.646): C: 62.53; H: 11.08. Found: C: 59.74; H: 11.32. ^{1}H NMR (C_6D_6); 1.06 (t, 18H, CH_3), 1.17 (s, 27H, CH_3), 1.76 (m, 9H, CH_2), 2.02 (m, 3H, CH_2); $^{13}C\{^1H\}$ NMR (C_6D_6) 11.29,11.52 (CH_2CH_3), 28.03, 28.29 ($C(CH_3)_3$), 29.10, 29.78 (CH_2), 38.84, 39.11 ($C(CH_3)_3$), 82.39, 84.90 (C).

$Gd(OCEt_2Bu^t)_3$. (**6**). Yield: 94%.

$La(OCEt_2Bu^t)_3$ (**7**). Yield: 92%. ^{1}H NMR (C_6D_6); 1.06 (t, 18H, CH_3) 1.14 (s, 27H, CH_3), 1.50–2.10 (m, 9H, CH_2); $^{13}C\{^1H\}$ NMR (C_6D_6) 11.01, 11.56 (CH_2CH_3), 27.86, 2.08 ($C(CH_3)_3$), 28.95, 29.39 (CH_2), 39.22, 39.60 ($C(CH_3)_3$), 84.05, 84.68 (C).

$Y(OCPr_3{}^i)_3$ (**8**). Yield: 95%. M.p. 262–270 °C. ^{1}H NMR (C_6D_6); 0.90, 1.11, 1.23 (d, 54H, CH_3), 2.15 (sept., 9H, CH); $^{13}C\{^1H\}$ NMR (C_6D_6) 20.04 (CH_3), 34.56 (CH).

$Gd(OCPr_3{}^i)_3$. (**9**). Yield: 93%.

$La(OC^iPr_3)_3$ (**10**). Yield: 92%. Anal. Calcd. for $La_1O_3C_{30}H_{63}$ (610.725): C: 59.00; H: 10.40. Found: C: 56.96; H: 10.40. ^{1}H NMR (C_6D_6); 0.91, 1.07, 1.16 (d, 54H, CH_3), 2.04 (sept., 9H, CH); $^{13}C\{^1H\}$ NMR (C_6D_6) 20.31 (CH_3), 34.76 (CH).

Single crystal X-ray diffraction

Earlier unknown crystal structures of $[Y(OCEt_2{}^tBu)_3]_2$ (**5**), $[La(OCEt_2{}^tBu)_3]_2$ (**7**), $[Gd(OC^iPr_3)_3]_2$ (**9**), and $[La(OC^iPr_3)_3]_2$ (**10**) were solved. Single crystals suitable for X-ray diffraction were crystallized from toluene solution. The crystals were mounted on a glass fiber with the viscous oil-drop method [23]. The equipment used was Bruker Nonius KappaCCD diffractometer (Mo Kα, $\lambda = 0.71073$ Å). Area-detector scaling and absorption corrections were done with a program SADABS [24]. Structures were solved and refined with the SHELX97 [25] software package. All non-hydrogen atoms were refined anisotropically; H atoms were calculated according to the ideal geometry. Illustrations were produced by the SHELXTL [26] program. Structures of **9** and **10** display rather large atomic displacement factors at terminal atoms. Several different models were tested for those atoms but agreeable solution was not found. Also, in all structures the differences between carbon atoms having the largest and the smallest thermal parameters are quite large. The latter can be explained by the presence of chemically very different carbon atoms in the structures. However, we consider these models chemically reasonable and describing best the actual crystal structures. Table 1 presents the summary of crystal data, data collection, and refinement parameters. CCDC reference numbers 812471–812474.

ALD studies

Thin films were grown by ALD using alkoxides 1, 2, 3, and 10 and water in a hot-wall flow-type commercial ALD reactor F120 [27] (ASM Microchemistry Ltd). Soda lime glass or silicon substrates (14 Ωcm) were used. The alkoxide precursors were assumed to be sensitive to air and moisture contamination and were loaded into the reactor using a special reservoir locked under argon. In order to suppress possible reactions with air moisture La_2O_3 films were covered with Al_2O_3 capping layer using ALD cycles of $Al(CH_3)_3$ and H_2O. The refractive indices and thicknesses of the films exceeding 50 nm and grown on glass substrates were evaluated from the transmission spectra measured by a Hitachi U2000 spectrophotometer [28]. The film structure was determined using Bruker D8 Advance X-ray diffractometer in grazing incidence mode (incidence angle 1°).

Results and discussion

Ten RE alkoxides with three different ligands and four RE elements were synthesized. RE ions with different sizes, i.e., Y^{3+} (0.900 Å/CN = 6), La^{3+} (1.032 Å/CN = 6), Pr^{3+}

Table 1 Crystal data and structure refinement for $[Y(OCEt_2{}^tBu)_3]_2$ (**5**), $[La(OCEt_2{}^tBu)_3]_2$ (**7**), $[Gd(OC^iPr_3)_3]_2$ (**9**), and $[La(OC^iPr_3)_3]_2$ (**10**)

Compound	**5**	**7**	**9**	**10**
Empirical formula	$Y_2O_6C_{54}H_{114}$	$La_2O_6C_{54}H_{114}$	$Gd_2O_6C_{60}H_{126}$	$La_2O_6C_{60}H_{126}$
Formula weight/g mol^{-1}	1032.23	1137.27	1258.11	1221.43
Temperature/K	173(2)	173(2)	173(2)	173(2)
Wavelength/Å	0.71073 (Mo Kα)			
Crystal system	Orthorhombic	Triclinic	Monoclinic	Monoclinic
Space group	*Pbca* (no. 61)	*P*-1 (no. 2)	$P2_1/c$ (no. 14)	$P2_1/n$ (no. 14)
Unit cell dimensions/Å, °	$a = 41.748(8)$	$a = 11.661(2)$	$a = 11.657(2)$	$a = 11.736(2)$
		$\alpha = 118.70(2)$		
	$b = 11.968(2)$	$b = 11.877(2)$	$b = 24.846(5)$	$b = 20.604(4)$
		$\beta = 90.33(4)$	$\beta = 112.39(3)$	$\beta = 104.17(3)$
	$c = 23.625(5)$	$c = 12.363(6)$	$c = 12.156(2)$	$c = 13.962(3)$
		$\gamma = 93.28(3)$		
Volume/Å^3	11804(4)	1498.3(8)	3255.3(11)	3273.4(11)
Z	8	1	2	2
Density (calculated)/Mg m^{-3}	1.167	1.260	1.284	1.239
Absorption coefficient/mm^{-1}	1.998	1.447	2.062	1.330
$F(000)$	4,511	600	1324.0	1296.0
Crystal size/mm^3	0.40 × 0.40 × 0.40	0.38 × 0.32 × 0.22	0.20 × 0.16 × 0.04	0.11 × 0.10 × 0.09
Theta range for data collection/°	5.02–27.54	5.00–25.00	5.01–27.60	5.03–25.85
Index ranges	$-54 \le h \le 54$	$-13 \le h \le 13$	$-15 \le h \le 14$	$-14 \le h \le 14$
	$-15 \le k \le 15$	$-14 \le k \le 13$	$-32 \le k \le 32$	$-25 \le k \le 25$
	$-30 \le l \le 30$	$-14 \le l \le 14$	$-15 \le l \le 15$	$-17 \le l \le 16$
Reflections collected	138,270	22,237	48,416	39,558
Independent reflections	13,488	5,227	7,369	6095
reflections with $I > 2\sigma(I)$	9,898	3,718	4,999	3,413
Completeness to θ/°	27.54° = 98.9%	25.00° = 99.0%	27.60° = 97.6%	25.85° = 96.3%
Refinement method	Full-matrix least-squares on F^2			
Data/restraints/parameters	13,488/10/588	5,227/0/295	7,369/115/325	6,095/54/325
Goodness-of-fit on F^2	1.038	1.008	1.098	1.064
R_{int}	0.0798	0.1375	0.0679	0.0919
R_1 indices $[I > 2\sigma(I)]$[a]	0.0502	0.0596	0.0580	0.0601
wR_2 indicecs $[I > 2\sigma(I)]$[b]	0.1035	0.0833	0.1538	0.1381
R_1 indices (all data)[a]	0.0814	0.1018	0.0920	0.1326
wR_2 indices (all data)[b]	0.1159	0.0920	0.1729	0.1683
Largest diff. hole and peak/e Å^{-3}	−0.896 and 1.789	−0.747 and 0.888	−0.656 and 1.222	−0.675 and 0.911

[a] $R_1 = \Sigma||F_o| - |F_c||/|F_o|$; [b] $wR_2 = [\Sigma w(F_o{}^2 - F_c{}^2)^2/\Sigma w(F_o{}^2)^2]^{1/2}$

(0.99 Å/CN = 6), and Gd^{3+} (0.938 Å/CN = 6) were chosen for this study [29]. The synthesis was done using the reaction of the appropriate silylamide with three equivalents of the appropriate alcohol. This frequently used method is the most effective and versatile route for the production of pure $RE(OR)_x$ compounds [30]. Two of the compounds, $Y(OCMe_2{}^iPr)_3$ and $La(OCMe_2{}^iPr)_3$, have been reported earlier by Bradley et al. [17] They used the same method for synthesis. These compounds and their preparation seem to be extremely sensitive to air and moisture. Visually there is no dramatic change in the compounds when they are affected by small amounts of moisture or air but the properties do change. Under inert atmosphere and rigorous air and moisture exclusion these compounds may be stored for months, at least.

NMR spectra were only measured for the diamagnetic compounds of yttrium and lanthanum. Praseodymium and gadolinium complexes are paramagnetic which makes it quite impossible to measure and interpret the NMR spectra. For yttrium and lanthanum complexes with 2,3-dimethyl-2-

butoxo ligand ^{1}H NMR reveal peaks shifted to lower field if compared to free ligand 2,3-dimethyl-2-butanol (^{1}H ($CDCl_3$): 0.83 (6H,d, CH_3), 0.98 (6H, s, CH_3), 1.47 (1H, septet, CH)). Peaks of the lanthanum compound are at lower field than those of the yttrium compound. ^{13}C spectra show one peak for each different carbon atom, i.e., four peaks are slightly shifted to a lower field if compared to the free alcohol. ^{1}H NMR spectra of yttrium and lanthanum compounds with the ligand ^{i}Pr$_3$CO$^-$ show three distinct doublets due to the isopropyl CH_3 protons while for CH only one septet is seen. Size relation of the three doublets is approximately 1:4:1. There are obviously three different environments around the CH_3 groups. However, ^{13}C NMR shows only three peaks due to three different carbon atoms. ^{1}H NMR spectrum for the yttrium and lanthanum compounds with the ligand ^{t}BuEt$_2$CO$^-$ shows a triplet due to the ethyl CH_3, singlet due to the *tert*-butyl CH_3, and two overlapping multiplets due to the ethyl CH_2. For some reason ^{13}C NMR spectrum shows two peaks for each different carbon atom.

Mass spectra was successfully measured only for the compounds with the 2,3-dimethyl-2-butoxo ligand (**1**–**4**). Only one major peak that contained the metal atom was seen for Y, Pr, and La compounds. This peak is associated with a dimeric species which has lost one ligand, i.e., $[M_2L_5]^+$. In the case of **2** some other metal containing fragment ions were also observed (see experimental). Other peaks observed were due to the alkoxo ligands and their fragments. These mass spectra are similar with those reported by Bradley et al. [17].

Crystallization of all the alkoxides prepared was tried but crystals suitable for single crystal XRD and reasonable structure solution were only found for four compounds: $[Y(OCEt_2{}^tBu)_3]_2$ (**5**), $[La(OCEt_2{}^tBu)_3]_2$ (**7**), $[Gd(OC^iPr_3)_3]_2$ (**9**), and $[La(OC^iPr_3)_3]_2$ (**10**). All four solved crystal structures are new and consist of dimeric molecules. Both metal atoms of the dimer are four coordinated and bonded to two terminally coordinated alkoxo ligands and two bridging alkoxo ligands. Coordination sphere of the metal atoms may be described as tetrahedral. There are only a few crystal structures of pure alkoxides of trivalent RE elements reported where the molecules are dimeric and the RE cations are four coordinated. Such compounds are $[Ce(OCH^tBu_2)_3]_2$ [31], $[La(OCPh_3)_3]_2$ [32], and $[Ce(OC^tBu_3)_2(O^tBu)]_2$ [33]. Two dimeric alkoxides with donor-functionalized alkoxo ligands namely $[Nd(OCMe_2CH_2CH_2OMe)_3]_2$ [34] and $[Lu(OCMe_2CH_2CH_2\ OMe)_3]_2$ [35] have been reported. Dimeric RE alkoxides with ancillary ligands (Lewis base adducts) are more common. Monomeric RE alkoxides are also known [30]. These are compounds with bulky alkoxo ligands and ancillary Lewis base ligands or compounds with bulky donor-fictionalized alkoxo ligands. It is unfortunate that structures of the alkoxides with the smallest alkoxo ligand ^{i}PrCMe$_3$O$^-$ could not be solved as these compounds have the best volatility.

Structure of $[Y(OCEt_2{}^tBu)_3]_2$ (**5**) (Fig. 1) was solved in the orthorhombic space group *Pbca* (no. 61) and the asymmetric unit is one molecule. Yttrium to oxygen bond distances in the molecule are 2.050(2)–2.065(2) Å for the oxygen atoms of the terminal alkoxo ligands, and 2.261(2)–2.278(2)Å for the oxygen atoms of the bridging alkoxo ligands. These distances are comparable with Y–O distances in other known yttrium alkoxide structures with terminal and μ_2-bridging alkoxo ligands [36]. For example in Y_2(9-methyl-9-fluorenoxy)$_6$(9-fluorenone) Y–O distances are 2.028–2.091 Å for the terminal alkoxo ligands and 2.227–2.301 Å for the bridging ligands [37]. The Y(1) to Y(2) distance is 3.591(1) Å.

Structure of $[La(OCEt_2{}^tBu)_3]_2$ (**7**) (Fig. 2) was solved in the triclinic space group *P*-1 (no. 2) and the asymmetric unit is half of the molecule. La to O bond distances for the terminal alkoxo ligands are 2.169(4) and 2.170(4) Å. La to O distances in the case of bridging alkoxo ligands are 2.436(4) and 2.437(4) Å. The distance between the two La atoms is 3.865(2) Å. The distances are again in line with distances observed earlier for La to O [32, 38]. In dimeric four coordinate lanthanum alkoxide $[La(OCPh_3)_3]_2$ La–O bond distances are 2.175–2.184 Å for the terminal ligands and 2.390–2.483 Å for the bridging ligands [32].

$[Gd(OC^iPr_3)_3]_2$ (**9**) (Fig. 3) crystallizes in the monoclinic space group $P2_1/c$ (no. 14). Only a half of the molecule has to be determined and the other half is generated through symmetry. The Gd to O distances for the terminal alkoxo ligands are 2.084(4) and 2.096(4) Å. In the case of the bridging alkoxo ligands the distances are 2.327(4) and 2.334(4) Å. The distance between the Gd atoms is 3.671(1) Å. Known gadolinium alkoxide structures with terminal and μ_2-bridging alkoxo ligands have Gd–O distances like 2.048–2.114 Å for terminal and 2.233–2.320 Å for bridging ligands in $Gd_5O(O^iPr)_{13}$ [39] and 2.276–2.295 Å for bridging ligands and 1.976–2.070 Å for terminal ligands in $Gd_2Cp_2(OCMe_2{}^iPr)_4$ [40].

$[La(OC^iPr_3)_3]_2$ (**10**) (Fig. 4) crystallizes in the monoclinic space group $P2_1/n$ (no. 14) and only half of the molecule has to be determined while the other half is generated through symmetry. The La to O distances in the case of terminal alkoxo ligands are 2.168(5) and 2.191(5) Å. The La to O distance for the bridging alkoxo ligands are 2.463(5) and 2.472(5) Å. La atoms are 3.925(1) Å distance away from each other. When compared with the $[La(OCEt_2{}^tBu)_3]_2$ (**7**) there is slight elongation of the La–O bond distances which may be interpreted to be due to a larger sterical hindrance. When compared with the dimeric four coordinate lanthanum alkoxide $[La(OCPh_3)_3]_2$ the La–O distances are similar [32].

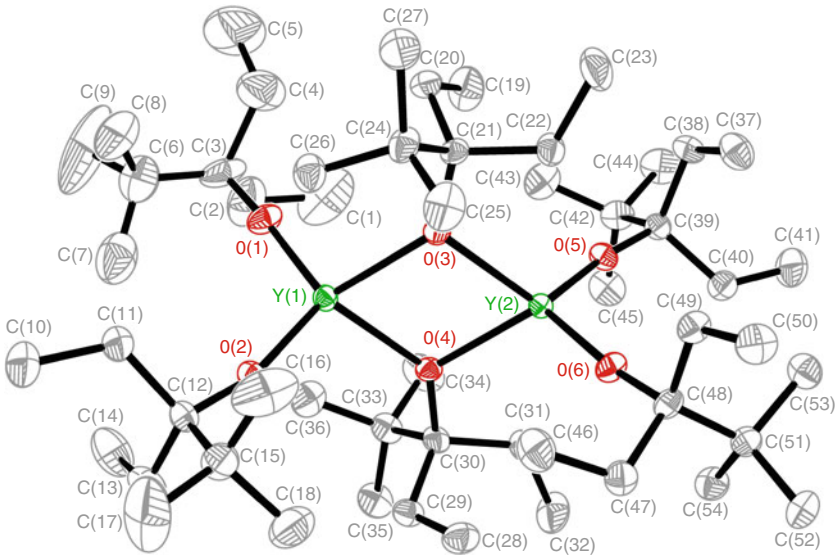

Fig. 1 Molecular structure of $[Y(OCEt_2{}^tBu)_3]_2$ (**5**). Hydrogen atoms are omitted for clarity and thermal ellipsoids are at 50% level

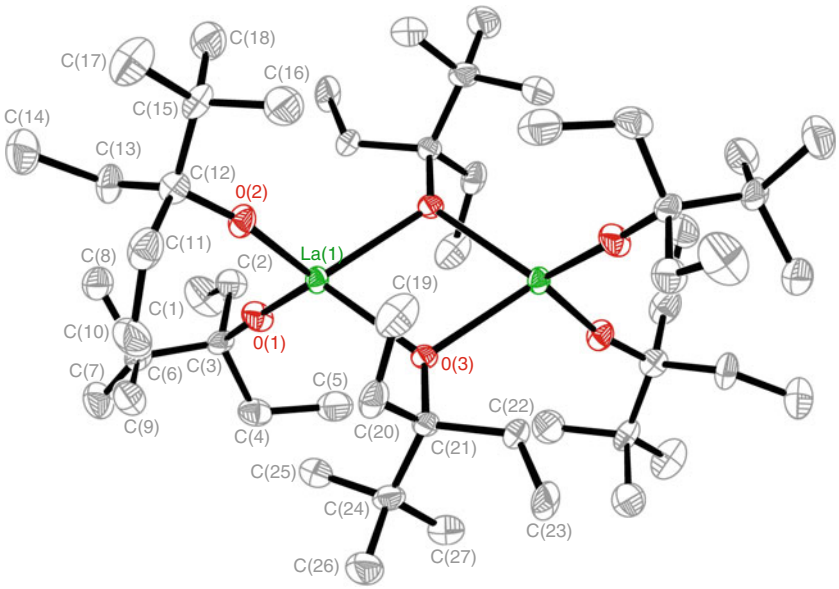

Fig. 2 Molecular structure of $[La(OCEt_2{}^tBu)_3]_2$ (**7**). Hydrogen atoms are omitted for clarity and thermal ellipsoids are at 50% level

Thermal analysis

All the compounds prepared were studied with simple dynamic TG measurement. The curves measured are shown in Figs. 5, 6, and 7. Some of the results may have been affected by the high air and moisture sensitivity of the samples. Samples were otherwise handled in inert gas atmosphere but loading into the TG equipment was done in air.

For the three yttrium compounds the TG and SDTA curves are shown in Fig. 5. $Y(OCMe_2{}^iPr)_3$ (**1**) and $Y(OCEt_2{}^tBu)_3$ (**5**) have one major step of weight loss. Complex **1** shows slow weight decrease of 4.3% up to 175 °C. After that starts a major step ($T_{50\%}$ = 296 °C) during which 83% of the sample weight is lost. At 600 °C the residue is 12.7%. SDTA reveals endotherms due to melting of the sample at 164–171 °C and evaporation. In the literature melting point of 161 °C has been given [17]. At the end of the evaporation the sample seems to generate some heat as an exotherm peak is observed. Complex **5** looses 1.3% of the weight up to 200 °C. In the following major step ($T_{50\%}$ = 350 °C) 76.9% of the weight is lost. The final residue at 600 °C is 21.7%. SDTA reveals three endothermic peaks. The first one is at 77 °C. Reason for this is unclear but it could be due to some solid phase transformation. The second endothermic peak at 212–216 °C is due to melting and the third around 354 °C due to evaporation. Again at the end of the weight loss (369 °C) an exotherm is seen. $Y(OC^iPr_3)_3$ (**8**) starts to lose weight already below 100 °C and the rate of the weight loss increases up to 270 °C. Between 270 and 380 °C the rate of weight loss is approximately constant. The residue

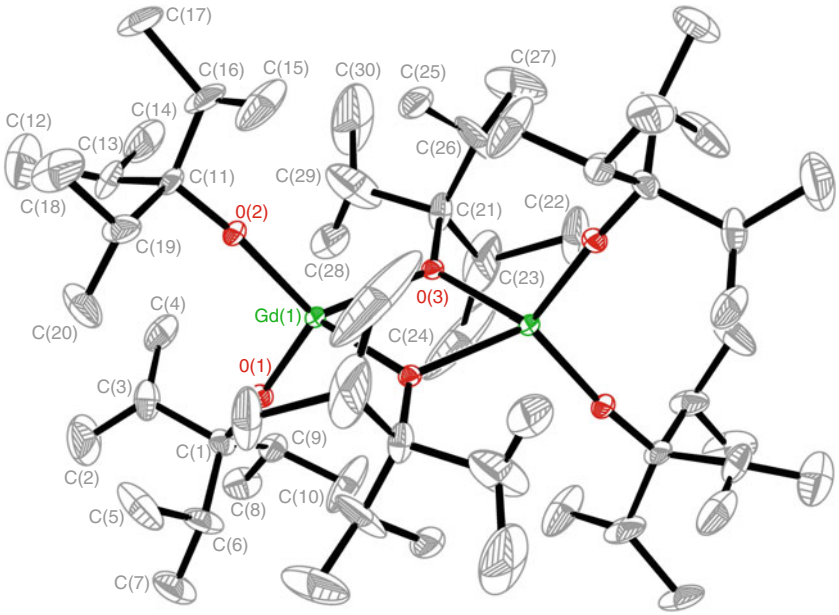

Fig. 3 Molecular structure of $[Gd(OC^iPr_3)_3]_2$ (**9**). Hydrogen atoms are omitted for clarity and thermal ellipsoids are at 20% level

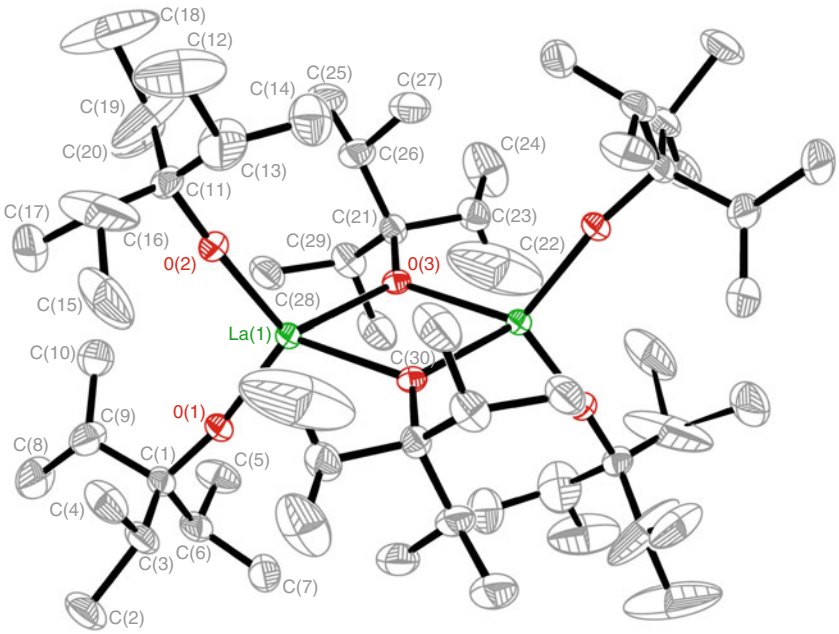

Fig. 4 Molecular structure of $[La(OC^iPr_3)_3]_2$ (**10**). Hydrogen atoms are omitted for clarity and thermal ellipsoids are at 20% level

at 600 °C is 15.9%. In SDTA an endotherm assigned for melting is seen at 262–270 °C. At the end of the weight loss there is an exothermic effect/process. The large residues seen in Fig. 5 indicate that the compounds mainly decompose. It could be assumed that the compounds decompose into Y_2O_3 or some other yttrium containing compounds. Theoretical amounts of Y_2O_3 that could form are 28.8, 21.8, and 20.1% for **1**, **5**, and **8**, respectively. Yttrium contents of the three compounds are 22.7, 17.1, and 15.9% for **1**, **5**, and **8**, respectively. In the case of **5** the residue is very close to the theoretical Y_2O_3 amount. In the case of **8** the residue is smaller and some yttrium containing species may have been evaporated. However, the shape of the curve is untypical for clear evaporation of a compound. In the case of **1** the observed residue is clearly smaller than the theoretical Y_2O_3 content (12.7 vs. 28.8%) which indicates that part of the compound has evaporated. For **1** also the temperature of the weight loss is the lowest among the yttrium alkoxides studied.

TG curves of the gadolinium alkoxides **2**, **6**, **9**, and $Pr(OCMe_2{}^iPr)_3$ (**4**) are shown in Fig. 6. All four alkoxides begin to lose weight slowly immediately show starting from the beginning a slowly descending weight. $Gd(OCMe_2{}^iPr)_3$ (**2**) shows only one major step of weight loss

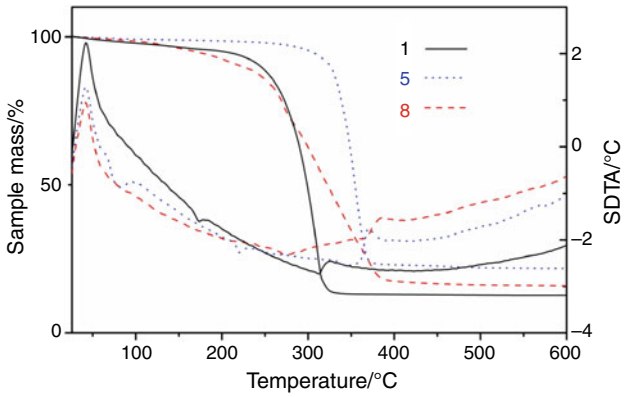

Fig. 5 TG and SDTA curves measured for yttrium alkoxides $Y(OCMe_2{}^iPr)_3$ (**1**), $Y(OCEt_2{}^tBu)_3$ (**4**), and $Y(OC^iPr_3)_3$ (**7**)

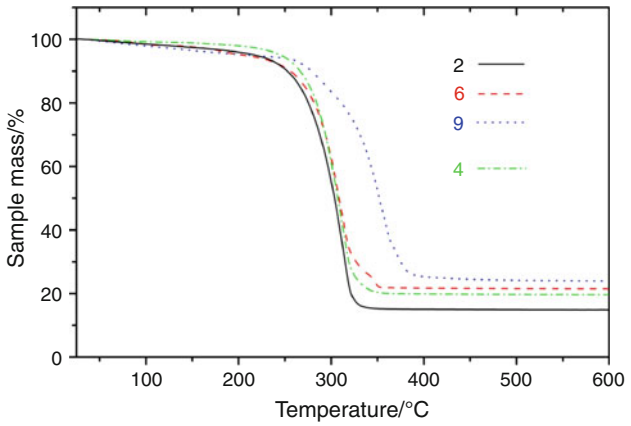

Fig. 6 TG curves of gadolinium and praseodymium alkoxides $Gd(OCMe_2{}^iPr)_3$ (**2**), $Gd(OCEt_2{}^tBu)_2$ (**6**), $Gd(OC^iPr_3)_3$ (**9**), and $Pr(OCMe_2{}^iPr)_3$ (**4**)

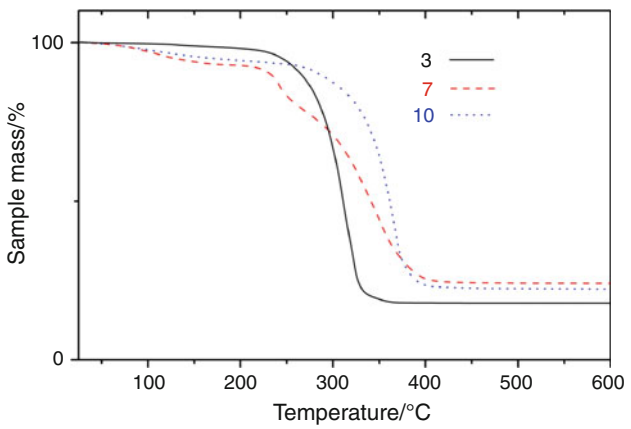

Fig. 7 TG curves of lanthanum alkoxides $La(OCMe_2{}^iPr)_3$ (**3**), $La(OCEt_2{}^tBu)_3$ (**7**), and $La(OC^iPr_3)_3$ (**10**)

starting around 200 °C and ending at 356 °C. The residue at 600 °C is 14.9% while the theoretical gadolinium content of the compound is 34.1% and the theoretical Gd_2O_3 residue that could form is 39.3%. Thus, it seems likely that during the step the compound partially evaporates and partially decomposes. In SDTA for some reason melting was not observed. Only an endotherm due to evaporation and subsequent exotherm were observed. $Gd(OCEt_2{}^tBu)_2$ (**6**) and $Gd(OC^iPr_3)_3$ (**9**) leave residues of 21.5 and 24.0%, respectively, while the theoretical amounts of Gd_2O_3 that could form are 30.9 and 28.8%, respectively. Theoretical Gd contents of **6** and **9** are 25.0 and 26.8%, respectively. For praseodymium only $Pr(OCMe_2{}^iPr)_3$ (**4**) was synthesized. This compound also looses weight in one major step between 150 and 370 °C ($T_{50\%}$ = 301 °C) and leaves a residue of 19.6% while the theoretical residue in case of Pr_2O_3 would be 37.1%. SDTA reveals an endotherm at 83–93 °C which is assigned to melting. As the residue is much smaller than the amount of Pr in the compound (31.7%) it is clear that a large part of the compound evaporates while some decomposition also takes place during the step of weight loss.

The behavior of the three alkoxides of lanthanum is quite similar to that of the Y and Gd analogs (Fig. 7). At first the weights are slowly descending. Then $La(OCMe_2{}^iPr)_3$ (**3**) and $La(OC^iPr_3)_3$ (**10**) show a single major step of weight loss at 210–370 °C ($T_{50\%}$ = 306 °C) and 265–450 °C ($T_{50\%}$ = 355 °C), respectively. In SDTA melting is seen for **3** only (m.p. 116–126 °C, lit. 119 °C [17]). Otherwise an endotherm due to evaporation and an exotherm at the end of the weight loss are seen. Residues left after the measurements were 17.9 and 22.3% while the theoretical La_2O_3 amounts in case of complete decomposition would be 36.8 and 26.7%. Theoretical La contents of **3** and **10** are 31.4 and 22.8%, respectively. TG curve of $La(OCEt_2{}^tBu)_3$ (**7**) shows three separable phases of weight loss. At first between 25 and 190 °C the sample looses 7.1% of the weight. Then between 190 and 268 °C ($T_{50\%}$ = 243 °C) the weight loss is 14.5% and after that 54.3% ($T_{50\%}$ = 229 °C). The weight change is complete around 450 °C. Residue at the end is 24.1% while in the case of decomposition to La_2O_3 the residue would be 28.7% (theoretical La content of **7** is 24.4%).

All the ten compounds could be sublimed under vacuum (150–220 °C/0.05 mbar) but the sublimation yields were quite modest (20–65%). We believe that the low yields are due to both the air and moisture sensitivity and partial thermal decomposition. The best yields were achieved with the 2,3-dimethyl-2-butoxy compounds.

Isothermal TG measurements were done with $La(OCMe_2{}^iPr)_3$ (**3**) to get information on evaporation rates at different temperatures and to detect possible decomposition. The results of these experiments are shown in Fig. 8, where the evaporation rate is represented in a logarithmic scale as a function of temperature. The linearity of this plot reflects the pure sublimation or evaporation in absence of thermal decomposition. The deviation from the linearity at

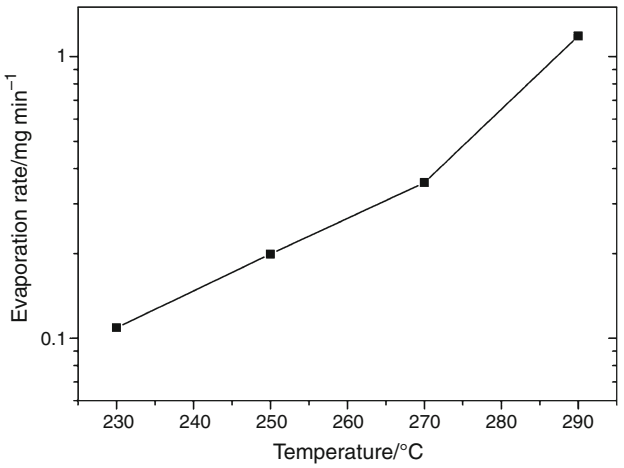

Fig. 8 Mass loss from La(OCMe$_2$C^{i}Pr)$_3$ (**3**) sample as function of temperature

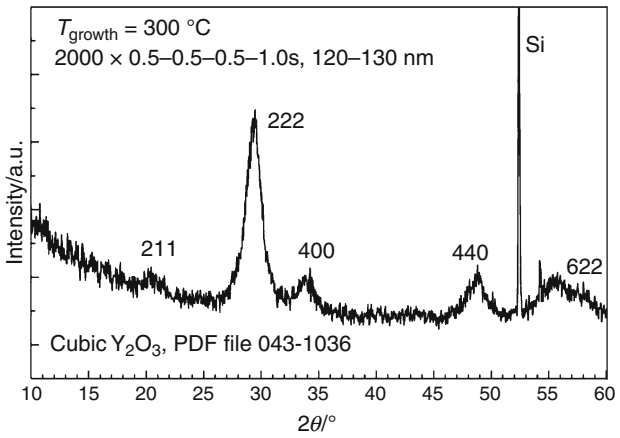

Fig. 9 Grazing incidence X-ray diffraction (incidence angle 1°) pattern of Y_2O_3 film on Si(100) grown at 300 °C from **1** and H_2O

290 °C is indicating most likely partial decomposition of the sample.

Overall the TG analysis revealed that the residue after the dynamic measurement was lower than the theoretical amount of RE oxide that could have formed in the case of all the alkoxides studied except one (compound **5** left residue approximately equal with the calculated Y_2O_3 amount). Also, the residues were smaller than the theoretical metal contents of the compounds for all compounds studied except two (compounds **5** and **7**). This indicates that in most cases partial evaporation of the metal containing compounds must have taken place. Another general observation is that while the alkoxides with ligand ^{i}PrMe$_2$CO$^-$ are the most volatile they also seem to be thermally the most unstable among the studied alkoxides, at least in the condensed phase.

ALD studies

The usage of Gd(OCMe$_2$^{i}Pr)$_3$ (**2**) for ALD of Gd_2O_3 with H_2O as the oxygen precursor was studied and reported by us already some years ago [19]. The results suggested self-limiting growth at quite high temperatures (350–400 °C), and considerable resistance of the precursor against thermal decomposition. Here we have tested compounds Y(OCMe$_2$^{i}Pr)$_3$ (**1**), La(OCMe$_2$^{i}Pr)$_3$ (**3**), and La(OC^{i}Pr$_3$)$_3$ (**10**) as ALD precursors.

Y_2O_3 films were deposited at 300 and 400 °C on soda lime glass and Si(100) substrates from Y(OCMe$_2$^{i}Pr)$_3$ (**1**) and H_2O. The cycle times used were 0.5–0.5–0.5–1.0 s and **1** was evaporated at 180 °C. The number of growth cycles applied at 300 and 400 °C were 2000 and 1500, resulting in films with thicknesses of 125 ± 5 and 157 ± 5 nm, respectively. These films were quite uniform, transparent, and possessing refractive index values 1.62 ± 0.01 and 1.53 ± 0.01, respectively, at 580 nm wavelength. XRD pattern measured for the Y_2O_3 film deposited at 300 °C (Fig. 9) reveals that the film is nanocrystalline. However, the structure of the films could be detected unambiguously. The bulk refractive index of Y_2O_3 should be in the range of 1.72–1.78, and the lowered value could be due to nanocrystallinity and impurities, causing relatively low density.

Growth of LaO_x films was tested with two lanthanum compounds, La(OCMe^{i}Pr)$_3$ (**3**) and La(OC^{i}Pr$_3$)$_3$ (**10**), with water as an oxygen precursor. The evaporation temperatures of **3** and **10** were 190 and 235 °C, respectively. In the case of **3** only two substrate temperatures, 250 and 300 °C, were examined. The precursor was found to be very sensitive to air and moisture and in order to achieve any film growth, the precursor had to be purified by sublimation procedure carefully. The thickness of resulting films occurred extremely nonuniform both along and across the gas flow direction. Precursor decomposition and/or the hydroxide formation were the likely reasons to the film thickness nonuniformity. The hydroxide formation occurs during the water pulse when water molecules react with the La_2O_3 film, and leads to thickness nonuniformity because the hydroxide is not stable but reacts with the lanthanum precursor during the next pulse [10]. Figure 10 shows the XRD pattern measured for LaO_x film in as-deposited state and after annealing at 750 °C under O_2 atmosphere.

For La(OC^{i}Pr$_3$)$_3$ (**10**) the substrate temperature range examined was 300–400 °C. The films were grown at 300, 350, and 400 °C using 1500, 2000, and 2000 cycles, respectively, and cycle times of 0.5–0.5–0.5–0.5 s. Film thicknesses measured were 440–600, 256–224, and 247–227 nm, respectively. The high film thicknesses, in particular that at the lowest temperature, is again most likely due to a formation of lanthanum hydroxide as an intermediate. It came out that the La precursor did not decompose essentially before 350 °C. At 375 °C and

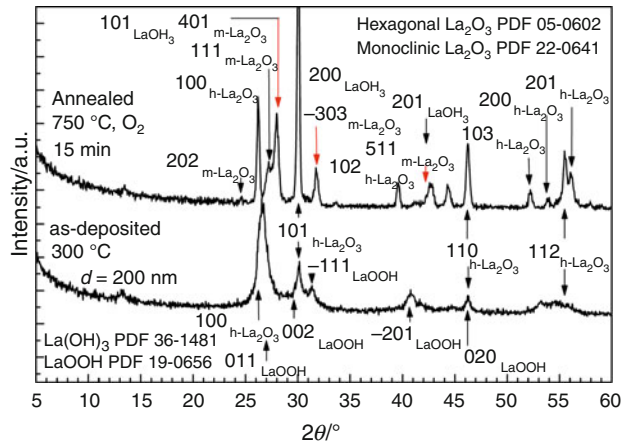

Fig. 10 Grazing incidence X-ray diffraction (incidence angle 1°) patterns of at least 200 nm thick LaO_x film grown from **3** and H_2O at 300 °C in as-deposited and annealed (750 °C) states. The LaO_x film is covered with at least 10 nm thick Al_2O_3 capping layer. Hexagonal phase is denoted by "h", monoclinic by letter "m"

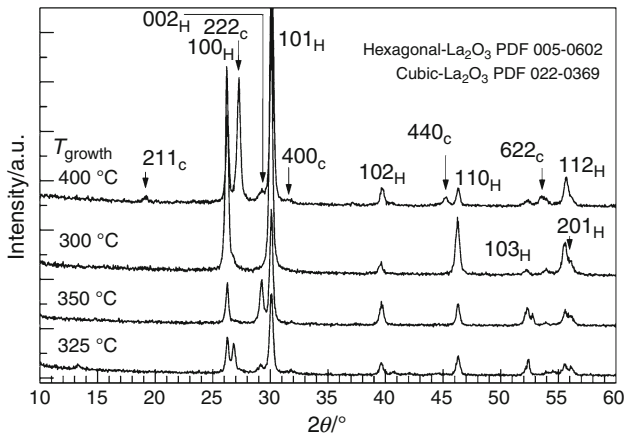

Fig. 11 Grazing incidence X-ray diffraction patterns of La_2O_3 films as-deposited at 300, 325, and 400 °C, respectively. Precursors used were **10** and H_2O

above, the decomposition became marked, resulting in dark substance and/or crystallites deposited on the reactor walls (glass tube) before reaching the substrate. The thickness nonuniformity remained an issue although the films grown from **10** were already more uniform than the films grown from **3**. Another important feature is the higher thermal stability of **10**, allowing growth at temperatures up to 350–375 °C, whereas **3** could effectively be used at around 300 °C only. The La_2O_3 films grown from **10** were crystalline already in as-deposited state. Most importantly, they did not reveal XRD peaks attributable to lanthanum hydroxides, as detected in the case of **3**, but rather two different La_2O_3 phases (cubic and hexagonal La_2O_3) as shown in the Fig. 11.

Anyhow, it appears that formation of lanthanum hydroxide at least as an intermediate severely complicates the growth process and leads to strong thickness nonuniformity when water is used as the oxygen source. While this seems to prevent exploitation of water in ALD of binary La_2O_3, the lanthanum alkoxide—water process should still be usable in ALD of ternary and mixed oxides like $LaAlO_3$ where the presence of the other oxide stabilizes the film against hydroxide formation [10].

Conclusions

A series of yttrium, lanthanum, praseodymium, and gadolinium alkoxides with tertiary alkoxo ligands was synthesized and characterized as possible precursors for ALD and CVD. Thermal properties of the compounds were studied with TG/SDTA. All of the alkoxides prepared showed quite large TG residues indicating thermal decomposition. However, in most cases the residues were smaller than the metal content of the compounds which indicates that decomposition was accompanied by some evaporation of the intact alkoxides. Among the alkoxides prepared the compounds with the ligand $^{i}PrCMe_2O^{-}$ were found to be the most volatile. Crystal structures were solved for $[Y(OCEt_2{}^{t}Bu)_3]_2$, $[La(OCEt_2{}^{t}Bu)_3]_2$, $[Gd(OC^{i}Pr_3)_3]_2$, and $[La(OC^{i}Pr_3)_3]_2$ and thus it has been clearly proven that these compounds are dimeric. It is unfortunate that the compounds with the smallest alkoxo ligand used in this study did not produce crystals suitable for structure solution. However, based on the volatilities it is expected that these compounds are also dimeric.

ALD studies with $Gd(OCMe_2{}^{i}Pr)_3$ and H_2O showed that ALD type growth of Gd_2O_3 occurred at temperatures between 250 and 400 °C though there were some problems with the repeatability of the results [19]. These problems were attributed to variation of the precursor quality due to very high air and moisture sensitivity. ALD tests with $Y(OCMe_2{}^{i}Pr)_3$ and H_2O were very promising at 300 °C. In the case of larger RE metal lanthanum ALD tests suggested that $La(OC^{i}Pr_3)_3$ is more suitable precursor than $La(OCMe^{i}Pr)_3$ due to its better thermal stability. Unlike the commonly used RE β-diketonates, RE alkoxides with tertiary alkoxo ligands presented here can be used to deposit RE oxides by ALD using water as the oxygen precursor. However, the usage of these RE alkoxides as ALD precursors is hampered by the sufficiently low thermal stability and extreme sensitivity to air and moisture.

References

1. Leskelä M, Ritala M. Rare-earth oxide thin films as gate oxides in MOSFET transistors. J Solid State Chem. 2003;171:170.

2. Leskelä M, Kukli K, Ritala M. Rare-earth oxide thin films for gate dielectrics in microelectronics. J Alloys Comp. 2006;418:27.
3. Leskelä M, Ritala M. Atomic layer deposition chemistry: recent developments and future challenges. Angew Chem Int Ed. 2003;42:5548.
4. Päiväsaari J, Niinistö J, Myllymäki P, Dezelah IV C, Winter CH, Putkonen M, Nieminen M, Niinistö L. Atomic layer deposition of rare earth oxides. In: Fanciulli M, Scarel G, editors. Topics in applied physics, vol. 106. Berlin, Heidelberg: Springer-Verlag; 2007. p. 15–32.
5. Aspinall HC. Requirements of precursors for MOCVD and ALD of rare earth oxides. In: Fanciulli M, Scarel G, editors. Topics in applied physics, vol. 106. Berlin, Heidelberg: Springer-Verlag; 2007. p. 33–72.
6. Niinistö J, Petrova N, Putkonen M, Niinistö L, Arstila K, Sajavaara T. Gadolinium oxide thin films by atomic layer deposition. J Cryst Growth. 2005;285:191.
7. Nieminen M, Putkonen M, Niinistö L. Formation and stability of lanthanum oxide thin films deposited from beta-diketonate precursor. Appl Surf Sci. 2001;174:155.
8. Potter RJ, Chalker PR, Manning TD, Aspinall HC, Loo YF, Jones AC, Smith LM, Critchlow GW, Schumacher M. Deposition of HfO_2, $Gd_2O_3$and PrO_x by liquid injection ALD techniques. Chem Vap Deposition. 2005;11:159.
9. Lim BS, Rahtu A, Gordon RG. Atomic layer depostion of transition metals. Nat Mater. 2003;2:729.
10. Lim BS, Rahtu A, deRouffignac P, Gordon RG. Atomic layer deposition of lanthanum aluminium oxide nano-laminates for electrical applications. Appl Phys Lett. 2004;84:3957.
11. Päiväsaari J, Dezelah CL, Back D, El-Kadri HM, Heeg MJ, Putkonen M, Niinistö L, Winter CH. Synthesis, structure, and properties of volatile lanthanide complexes containing amidinate ligands: application for Er_2O_3 thin film growth byatomic layer deposition. J Mater Chem. 2005;15:4224.
12. Putkonen M, Niinitö L. Organometallic precursors for atomic layer deposition in CVD precursors. Top Organomet Chem. 2005;9:125.
13. Bradley DC, Mehotra RC, Gaur DP. Metal alkoxides. London: Academic Press; 1978.
14. Poncelet O, Sartain WJ, Hubert-Pfalzgraf LG, Folting K, Caulton KG. Chemistry of yttrium triisopropoxide revisited—characterization and crystal-structure of $Y_5(\mu_5\text{-}O)(\mu_3\text{-}O^iPr)_4(\mu_2\text{-}O^iPr)_4(O^iPr)_5$. Inorg Chem. 1989;28:263.
15. Bradley DC, Chudzynska H, Frigo DM, Hammond ME, Hursthouse MB, Mazid MA. Pentanuclear oxoalkoxide clusters of scandium, yttrium, indium and ytterbium, x-ray crystal-structures of $[M_5(\mu_5\text{-}O)(\mu_3\text{-}OPr^i)_4\ (\mu_2\text{-}OPr^i)_4(OPr^i)_5]$ (M = In, Yb). Polyhedron. 1990;9:719.
16. Helgesson G, Jagner S, Poncelet O, Hubert-Pfalzgraf LG. Synthesis and molecular-structure of $Nd_5(\mu_5\text{-}O)(\mu_3\text{-}OR)_2(\mu_2\text{-}OR)_6(OR)_5(ROH)_2$ (R = Pr^i)—the 1st example of a trigonal bipyramidal metal oxoalkoxide. Polyhedron. 1991;10:1559.
17. Bradley DC, Chudzynska H, Hursthouse MB, Motevalli M. Volatile tris-tertiary-alkoxides of yttrium and lanthanum—the x-ray crystal-structure of $[La_3(OBu\text{-}tert)_9(Bu\text{-}tertOH)_2]$. Polyhedron. 1991;10:1049.
18. Anwander R. Routes to monomeric lanthanide alkoxides. In: Herrmann WA, editor. Topics in current chemistry, vol. 173. Berlin: Springer; 1996. p. 149.
19. Kukli K, Hatanpää T, Ritala M, Leskelä M. Atomic layer deposition of gadolinium oxide films. Chem Vap Deposition. 2007;13:546.
20. Buhler JD. Reaction of lithium alkyls with aldehydes and ketones—general study. J Org Chem. 1973;38:904.
21. Imamoto T, Takiyama N, Nakamura K, Hatajima T, Kamiya Y. Reactions of carbonyl-compounds with Grignard-reagents in the presence of cerium chloride. J Am Chem Soc. 1989;111:4392.
22. Bradley DC, Ghotra JS, Hart FA. Low coordination numbers in lanthanide and actinide compounds. 1. Preparation and characterization of tris[bis(trimethylsilyl)-amido]lanthanides. J Chem Soc Dalton Trans 1973:1021.
23. Kottke T, Stalke D. Crystal handling at low-temperatures. J Appl Crystallogr. 1993;26:615.
24. Sheldrick GM. SADABS, a software for empirical absorption correction. Gottingen, Germany: University of Gottingen; 2000.
25. Sheldrick GM. A short history of SHELX. Acta Crystallogr Sect A. 2008;64:112.
26. SHELXTL Reference Manual, Version 5.1; Bruker AXS, Analytical Instrumentation, Madison, Wisconsin, USA; 2000.
27. Suntola T. Atomic layer epitaxy. Thin Solid Films. 1992;216:84.
28. Ylilammi M, Ranta-aho T. Optical determination of the film thicknesses in multilayer thin-film structures. Thin Solid Films. 1993;232:56.
29. Shannon RD. Revised effective ionic-radii and systematic studies of interatomic distances in halides and chalcogenides. Acta Crystallogr Sect A. 1976;32:751.
30. Boyle TJ, Ottley LAM. Advances in structurally characterized lanthanide alkoxide, aryloxide, and silyloxide compounds. Chem Rev. 2008;108:1896.
31. Stecher HA, Sen A, Rheingold AL. Synthesis, structure, and reactivity of cerium(III) alkoxides. 2. Thermal-decomposition of $Ce(OCtBu_3)_3$ and the structure of $[Ce(OCHtBu_2)_3]_2$. Inorg Chem. 1989;28:3280.
32. Evans WJ, Golden RE, Ziller JW. A comparative synthetic and structural study of triphenylmethoxide and triphenylsiloxide complexes of the early lanthanides, including X-ray crystal-structures of $La_2(OCPh_3)_6$ and $Ce_2(OSiPh_3)_6$. Inorg Chem. 1991;30:4963.
33. Sen A, Stecher HA, Rheingold AL. Synthesis, structure, and reactivity of homoleptic cerium(IV) and cerium(III) alkoxides. Inorg Chem. 1992;31:473.
34. Gromada J, Morteux A, Chenal T, Ziller JW, Leising F, Carpentier J-F. Neodymium alkoxides: synthesis, characterization and their combinations with dialkylmagnesiums as unique systems for polymerization and block copolymerization of ethylene and methyl methacrylate. Chem Eur J. 2002;8:3773.
35. Anwander R, Munch FC, Priemeier T, Scherer W, Runte O, Hermann WA. Volatile donor-functionalized alkoxy derivatives of lutetium and their structural characterization. Inorg Chem. 1997;36:3545.
36. Allen FH. The Cambridge Structural Database: a quarter of a million crystal structures and rising. Acta Crystallogr B. 2002;58:380–8.
37. Dietrich HM, Meermann C, Tornroos KW, Anwander R. Sounding out the reactivity of trimethylyttrium. Organometallics. 2006;25:4316.
38. Aspinall HC, Bickley JF, Gaskell JM, Jones AC, Labat G, Chalker PR, Williams PA. Precursors for MOCVD and ALD of rare earth oxides-complexes of the early lanthanides with a donor-functionalized alkoxide ligand. Inorg Chem. 2007;46:5852.
39. Kritikos M, Moustiakimov M, Wijk M, Westin G. Synthesis, structure and characterisation of $Ln_5O(OPr^i)_{13}$ with Ln = Nd, Gd or Er. J Chem Soc Dalton Trans 2001:1931.
40. Daniel SD, Lehn J-SM, van der Heide P, Wang Y, Hoffman DM. Synthesis of cyclopentadienyl gadolinium and samarium alkoxide complexes. Inorg Chim Acta. 2006;359:257.